Biomacromolecules

December 2007 Published by the American Chemical Society Volume 8, Number 12

Communications

A High Strength Nanocomposite Based on Microcrystalline Cellulose and Polyurethane

Qiuju Wu, Marielle Henriksson, Xiaohui Liu, and Lars A. Berglund*

Fibre and Polymer Technology, Royal Institute of Technology, KTH, 100 44 Stockholm, Sweden

Received September 22, 2007; Revised Manuscript Received November 4, 2007

A high-strength elastomeric nanocomposite has successfully been prepared by dispersing microcrystalline cellulose in a polyurethane matrix. The resulting nanocomposites show increased strain-to-failure in addition to increased stiffness and strength compared to the unfilled polyurethane. The optimal composite contained 5 wt % cellulose. The average true strength for this composition was 257 MPa, compared with 39 MPa for the neat polyurethane, and showed the highest strain-to-failure. The improvements of stiffness, strength, as well as strain-to-failure are believed to be due to good interaction, by both covalent and hydrogen bonds, between the polyurethane and the cellulose nanofibrils.

Introduction

Polymer nanocomposites have attracted great interest during recent years. One reason is the potential for significant improvements in mechanical properties already at very small volume fractions of the reinforcing phase.[1] Examples of reinforcements include clay minerals and carbon nanotubes. In the context of biopolymer-based reinforcement, cellulose is of major interest because the experimentally measured axial Young's modulus of the cellulose crystal is 134 GPa.[2]

Cellulose has a major load-bearing function in many plants and is present in the form of microfibrils, consisting of aligned threadlike bundles of poly-β(1,4)-D-glucose molecules in extended-chain conformation.[3] In the microfibrils, the molecules are stabilized laterally by hydrogen bonds between hydroxyl groups and oxygens of adjacent molecules.[3] The small size of the typical lateral dimension (4–20 nm) combined with potential lengths of several μm provides very high aspect ratio at small scale. Cellulose microfibrils originate from renewable plant resources and may function as biodegradable nanofibrils in high-performance composites.

Favier et al. studied composites based on tunicin cellulose whiskers.[4] The whiskers are large aspect ratio crystals obtained from the mantle of tunicates, a type of edible sea animals. In cast films of styrene cobutyl acrylate latex composites, the tunicin whiskers formed a network at low concentration so that the small strain composite modulus showed drastic improvement in the rubbery state. Interestingly, Boldizar et al. much earlier used microcrystalline cellulose (MCC) as reinforcement in polymer composites.[5] MCC is obtained by acid hydrolysis of cellulosic fibers, and typical dimensions of dispersed MCC nanofibrils are 20 nm in diameter and around 200 nm in length.[6]

As the potential of polymer nanocomposites is considered, rubbery state effects are of particular interest. In a recent study, Cao et al.[7] prepared nanocomposites based on waterborne polyurethane (PU) and acid-hydrolyzed cellulose nanofibrils. The study emphasizes environmental advantages of caprolactone-based waterborne PU nanocomposites based on cellulose. In addition, interesting improvements in mechanical properties were reported. The present study is motivated by a desire to develop the understanding of reinforcement mechanisms in cellulosic nanocomposites. The study is an extended version of a more limited conference contribution,[8] to which new data and a qualified interpretation of reinforcement mechanisms have been added. The interpretation is stimulated by Cao's results[7] and a recent study by Sternstein and Zhu.[9] An interesting observation is that the present cellulose−PU nanocomposites show increased strain-to-failure with nanocellulose addition, in contrast with Cao's data as well as previous studies.[10] In addition, the reinforcement effect at low cellulose content is much stronger in the present material, and the reason for this is discussed.

* Corresponding author. E-mail: blund@kth.se. Telephone: +46-8-7908118. Fax: +46-8-7908101.

10.1021/bm701061t CCC: $37.00
Published on Web 11/21/2007

In general, good compatibility between the nanocellulose and the polymer matrix is essential because cellulose agglomeration otherwise becomes a problem.[5] For this reason, thermoplastic polyurethanes are favorable matrices due to their hydrophilic nature. The hydroxyl groups on the cellulose nanofibril surface may interact favorably with the PU.

Addition of fibers or fillers to PU leads to strong reinforcement effects[11–14] although often at the expense of reduced strain-to-failure. Nanoscale fillers may improve the balance between stiffness, strength, and strain-to-failure. Specially synthesized rigid polybenzamide nanowhiskers of approximately 2000 nm length and 200 nm diameter were reported to increase tensile strength and Young's modulus without sacrificing high strain-to-failure.[12] Recently, nanolayers of clay were applied as platelet reinforcement, resulting in enhanced polyurethane modulus, strength, and strain-to-failure.[15–18] Related to these encouraging results, the major objective of the present study is to prepare true cellulose nanocomposites based on a rubbery PU thermoplastic and investigate the reinforcement potential of microcrystalline cellulose, in particular at high strains.

Materials and Methods

Materials and Composite Preparation. Cellulose fiber (1–2 mm in length) was used for the preparation of polyurethane−cellulose conventional composites. Microcrystalline cellulose (Avicel PH105), delivered as a dry powder with 50 μm average particle size, was used in polyurethane−cellulose nanocomposites. Dimethylformamide (DMF, 99%, Fluka), 4,4′-diphenyl-methane diisocyanate (MDI, Aldrich), polytetramethylene glycol (PTMEG, M_n = 1000, DuPont), lithium chloride (99%, Sigma), and 1,4-butanediol (1,4-BG, Fluka) were used as received.

The pure polyurethane is synthesized following a previous route.[15] MDI (9 g) and PTMEG (18 g) at a molar ratio of 2:1 were dissolved in DMF solvent and then heated to 90 °C with stirring to form prepolymer. 1,4-BG (1.62 g) was added to the prepolymer with stirring at room temperature for 3 h to complete the reaction. The PU films were formed by casting the solution in a mold and then removing the solvent at 80 °C. Slow solvent evaporation was essential for the production of void-free films.

The conventional composite of polyurethane−cellulose was prepared as follows. Cellulose pulp fiber (5 wt %), MDI (9 g), and PTMEG (18 g) were mixed with DMF and then stirred and heated to 90 °C to form prepolymer. 1,4-BG (1.563 g) was added to the prepolymer with stirring at room temperature for 3 h. The product is termed PU/L-C5.

The preparation of polyurethane−cellulose nanocomposite is as follows; Different amounts of cellulose crystal and a trace amount (<0.3 wt %) of LiCl were mixed with DMF, kept stirring at 80 °C for 6 h, then MDI (9 g) and PTMEG (18 g) at 2:1 molar ratio were added. Prepolymer was obtained after stirring at 90 °C for 3 h. Then 1.600, 1.544, 1.541, and 1.541 g of 1,4-BG were added into the prepolymer systems with 1, 3, 5, and 10 wt % cellulose, respectively. The addition amount of 1,4-BG was determined by the measured amount of residual NCO groups in the prepolymer[19] in order to have a 1:1 molar ratio between NCO groups and accessible OH groups. It was based on quantitative analysis of the intense peak of NCO bond at 2270 cm^{-1} in the FT-IR spectrum. After stirring at room temperature for 3 h at and removal of solvent at 80 °C, elastic films were obtained. The final composites, containing 1, 3, 5, and 10 wt % cellulose, were termed PU/C1, PU/C3, PU/C5, and PU/C10, respectively.

Characterization. X-ray diffraction (XRD) patterns of the obtained films were recorded by a Siemens D5000 X-ray diffractometer at room temperature. The CuKα radiation source was operated at 40 kV and 40 mA. Patterns were recorded by monitoring diffractions from 1.5° to 30°. The scan speed was 2°/min.

The samples for transmission electron microscopy (TEM) study were first prepared by placing PU/cellulose into epoxy capsules, and the epoxy was cured at 70 °C for 24 h in a vacuum oven. Then the cured epoxies containing PU/cellulose were microtomed with a LKB Bromma 2088 ultrotome into 80–100 nm thickness. A carbon layer of 3 nm thickness was deposited on these slices on 200 mesh copper nets for TEM observation (JEOL-2000EX).

The FT-IR analyses were carried out using a Perkin-Elmer 2000 spectrometer. Approximately 10 μm thick films of the final polymers were applied in the FT-IR measurements. For analyzing the NCO content in the prepolymers, the KBr tablet method was used in the FT-IR measurements.

The tensile tests were carried out with an Instron 4411. Samples were cut to 100 × 10 × 1 mm^3 in size, and the crosshead speed was set at 100 mm/min. For each data point, five samples were tested and the average value was taken. The modulus was determined in the small strain region. Engineering stress, σ_{eng}, was calculated from $\sigma_{eng} = F/A_0$, where F was applied load and A_0 initial cross-sectional area. Engineering strain, ϵ_{eng}, was calculated from $\epsilon_{eng} = \Delta L/L_0$, where ΔL was the extension of the sample and L_0 was initial sample length. True stress, σ_{true}, was calculated from $\sigma_{true} = F/A$, where $A = A_0(L_0/L)$. True strain, ϵ_{true}, was calculated as $\epsilon_{true} = \ln(L/L_0)$. True stress and strain was calculated by assuming no change in sample volume during the test.[20]

Dynamic mechanical tests were performed on a DMTA Mark II spectrometer in tension mode. The specimen was a thin rectangular strip with dimensions of 10 × 5 × 1 mm^3. Measurements were performed in isochronal conditions at 1 Hz, and the heating rate was 2 °C/min.

Results and Discussion

Composites Preparation. Cellulose nanocomposites were produced from dispersed MCC nanofibrils and polyurethane monomers using a polymerization procedure in combination with solvent casting. The first step aimed for swelling of the MCC, although the swelling power of the solvent system must be tuned in order not to dissolve the cellulose. Partial polymerization of the isocyanate and the diol was carried out in the swollen state. A chain extender was added to the system in order to increase molar mass. At this state, the solvent served as a processing aid and allowed pouring of the material into a mold. Polymerization continued, and molar mass increased further. The solvent evaporated, and a smooth, solid nanocomposite film was obtained.

In the first swelling step, hydrogen bonding between the cellulose nanofibrils in the MCC particulate fillers was weakened by the solvent system, DMF combined with a small amount of LiCl. The purpose is to create nanofibrils of improved aspect ratio compared with the dried MCC particulate filler. As the monomers were added, they were able to enter into the swollen gel-like nanofibril system. As the material was subjected to 80 °C, polymerization commenced.

DMF and Li^+ play key roles in weakening hydrogen bonding between nanofibrils in the MCC. The interaction of lithium salts with polar aprotic solvents, such as DMF and DMAc, has been studied by means of various NMR and IR techniques.[21–24] When the concentration of lithium ions in DMAc is higher than 5 wt %, typically 8–9 wt %, cellulose can be dissolved, although the dissolution mechanism still remains unclear.[25,26] In the present work, the crystalline structure of cellulose must be maintained so that the nanofibrils are not dissolved. Therefore only trace amounts (<0.3 wt %) of lithium chloride is used. A proper balance is aimed for so that the solvent system can swell the MCC although maintaining the crystalline structure of the nanofibrils.

If we consider the function of DMF, it has been reported that the NH_2 group can weaken the interchain hydrogen bonding in cellulose, forming a new hydrogen bonding structure like

Figure 1. TEM image of PU/C5.

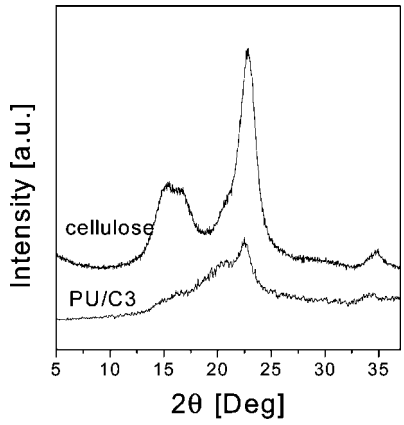

Figure 2. XRD patterns of cellulose and PU/C3.

O—H···N between the hydroxyl group on the cellulose and the N atom on the NH_2 group.[27] After such treatment with high concentrations of LiCl, the fibril bundles are swollen, as shown by Davis et al.[28] The [101] interplanar distance of the unit cell increased from 1.03 nm for pristine cellulose to 2.87 nm of $C_7H_{15}NH_2$-treated cellulose. A chelate structure involving cellulose, DMF, and Li^+ is believed to strengthen and accelerate the swelling process due to its stable structure and strong steric effect.[29] The fibril bundles are loosened and allow the monomer to enter into the space between fibrils. The nucleophilic OH group in cellulose could attract a strongly electrophilic isocyanate monomer (MDI). During polymerization, MDI could react with the OH groups both at the cellulose nanofibril surfaces and in the diol (PTMEG) chains.

Nanocomposite Structure. After preparation of cellulose nanocomposite films, it was essential to confirm that the cellulose nanofibrils and the cellulose I structure were preserved. The morphology of the nanocomposite was studied by transmission electron microscopy (TEM) (Figure 1). Cellulose nanofibrils, approximately 20–40 nm in diameter and with considerable aspect ratio, are apparent and dispersed in the polyurethane matrix. The presence of nanofibrils in the TEM micrograph supports successful isolation without dissolution of the cellulose.

The X-ray diffraction (XRD) spectra for MCC (cellulose) and the nanocomposite with cellulose content of 3 wt % (PU/C3) are presented in Figure 2. The peak at 22.7° is characteristic for cellulose I.[30] Despite low cellulose content, the peak is clearly visible also in PU/C3. This provides additional evidence that the original crystalline structure of cellulose (cellulose I) is still present in the nanocomposite. The crystalline cellulose I form will change to cellulose II after regeneration from a strong 8% LiCl/DMAC solution. Instead, cellulose dissolution is avoided with the poor solvent system in the present study. Most likely, nanofibril surfaces and disordered regions are swollen, without any influence on the interior of crystalline regions.

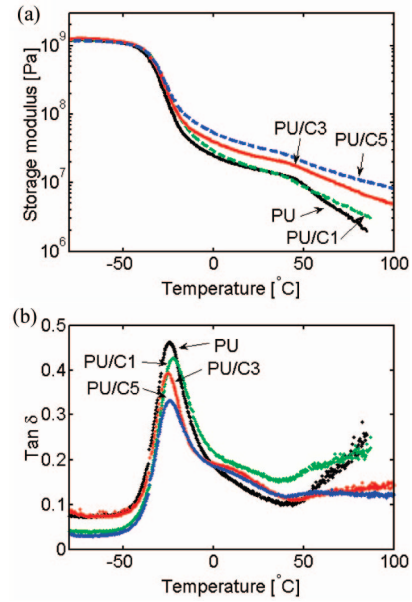

Figure 3. Storage modulus (a) and tan δ (b) vs temperature at 1 Hz for polyurethane and polyurethane−cellulose composites.

Nanocomposite Properties. Dynamic mechanical thermal analysis was performed on pure PU, PU/C1, PU/C3, and PU/C5 with cellulose contents of 0, 1, 3, and 5% by weight, respectively. In the pure polyurethane (Figure 3a), the modulus remains almost constant at temperatures below T_g. A rapid decrease in tensile modulus is then observed at the glass–rubber transition. In the rubbery region, the tensile modulus keeps decreasing with temperature due to the thermoplastic nature of the material. Above T_g, a significant modulus increase is observed in the nanocomposites, although the cellulose content is only a few percent. For instance, the modulus at 5 °C of a film containing 5 wt % cellulose is approximately 200% of the matrix material, while at 85 °C, it is approximately 500%. Compared with the acrylate latex−tunicin whisker composite studied by Favier et al.,[4] the rubbery state reinforcement effect is lower. Their data are based on a specific effect due to the formation of a paperlike fibrous network. The formation of such a network at low reinforcement content requires high aspect ratio fibrils and strong fibril−fibril interaction. In the present case, there is no fibril network and the fibril aspect ratio is not as high as with tunicate whiskers. There is a slight reinforcement effect on the apparent softening "knee" of the neat PU at around 50 °C.

A slight decrease in the tan δ peak at T_g is observed with increasing cellulose content (Figure 3b). Apparently, a smaller proportion of the matrix participates in the glass transition when nanodispersed nanofibrils are present. This indicates favorable matrix−fiber interaction and possibly the formation of an interphase matrix layer, either immobilized or of reduced molecular mobility.[31] In a previous study,[32] a stronger decrease in tan δ peak was observed in a thermoplastic polyester−tunicin whisker composite. Although such effects obviously depend on

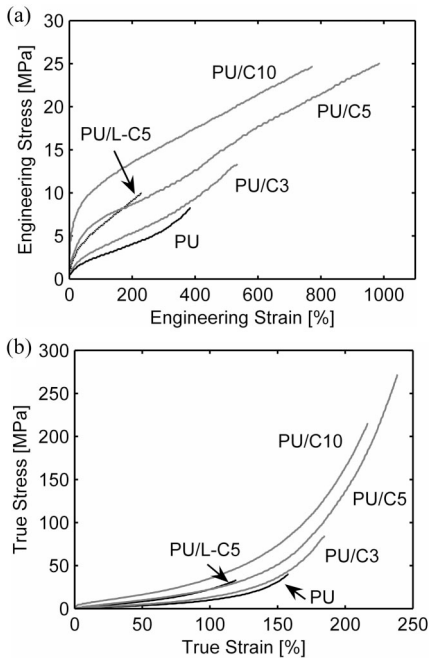

Figure 4. Engineering stress–strain curves (a) and true stress–strain curves (b) for polyurethane and polyurethane−cellulose composites.

specific cellulose−polymer matrix interactions, the cellulose nanofibril surface is likely to show high molecular order, which facilitates matrix interaction.

No consistent T_g shift is observed in the nanocomposites as compared with the pure polyurethane (Figure 3b). The addition of lithium salt to polyurethane may result in increased T_g[33] and reduced elastomeric properties,[34] although the present lithium salt content seems too low for such an effect. A final observation from Figure 3b is that the relaxation peak of the PU matrix at around 60 °C is weakened in the nanocomposite specimens.

The nanocomposites prepared for uniaxial tensile tests contained 3, 5, and 10 wt % of cellulose and were termed PU/C3, PU/C5, and PU/C10. The conventional composite with 5 wt % cellulose was termed PU/L-C5. Typical stress–strain curves are shown in Figure 4. The data for tensile strength, tensile modulus, and strain-to-failure are summarized in Table 1. In the conventional PU/L-C5 composite, modulus and strength increase, whereas strain-to-failure decreases significantly. This is common for polyurethane composites reinforced by conventional microscale fillers.[12–14,35] In general, the reason for low strain-to-failure in microcomposites is failure initiation by interfacial debonding at multiple sites followed by debond crack coalescence and catastrophic crack growth.[36,37]

In the nanocomposites, tensile strength, tensile modulus, and strain-to-failure are increased as compared with the neat PU. The tensile modulus increases with the cellulose content, reaching the highest value of 21 MPa at 10 wt % cellulose, 4 times higher than for the matrix. The strain-to-failure is increased in all three nanocomposites. The largest improvement occurs in PU/C5 (true strain-to-failure 1.5 times higher than for the matrix). The true tensile strength increases by more than a factor of 6 for the PU/C5 composition (Table 1).

The shape of the engineering stress–strain curves is in the form of an initial steep region followed by a highly curved nonlinear region, which has reached an approximately constant slope at around 100% engineering strain. At this strain, the stress level is increased with increasing cellulose content. Since engineering stress–strain curves above 100% strain are roughly parallel for the nanocomposites, ultimate strength correlates with ultimate strain.

In the nanocomposites, the enhancement in strength and modulus is directly attributable to the reinforcement provided by cellulose nanofibrils dispersed at the nanoscale. At the same cellulose content, the PU/C5 nanocomposite shows higher modulus, higher strength, and higher strain-to-failure than the conventional PU/L-C5 composite.

Curves of true stress versus true strain in Figure 4b provide additional insight into deformation mechanisms. Above 150% true strain, the stress–strain slope becomes steeper and the PU/C5 composite fails at a stress of 257 MPa. The stiffening effect at high strains is due to a combination of preferred molecular and nanofibril orientation in the loading direction. It is also interesting to note that in the mid range of strains, the microcomposite PU/L-C5 is not so different from PU/C5 in this type of plot.

Interfacial interaction between cellulose and the polyurethane matrix is a factor contributing to the observed reinforcements effects. FT-IR studies of the prepolymer show a lowered NCO-peak in the composites as compared with in the neat PU. The NCO peak is associated with end groups in the prepolymer. The lowered NCO concentration indicates that some surface hydroxyls in cellulose react with MDI, serving as a nucleophilic reactant. On the basis of this assumption and the lowered NCO concentration, about 5% MDI is estimated to react with cellulose in the composites. In practice, only cellulose at nanofibril surfaces is likely to be accessible for chemical reaction. This indicates that a large proportion of the hydroxyl groups at the nanofibril surfaces do indeed react with MDI. Cellulose nanofibrils are then covalently bonded to the ends of some polymer chains. Another indication that MDI−cellulose reactions occur is an observation made during development of the composite preparation procedure. If the time between mixing of MDI−cellulose and the casting event was too long, a gel formed. Similar conditions for the neat PU system did not result in a gel. This indicates that cellulose strongly interacts with the PU matrix. It is worth noting that the ratio of NCO groups/−OH groups was kept constant in all samples.

The cellulose nanocomposite reinforcement effect on polyurethane may possess one or more effects in common with those discussed for carbon black.[38] Detailed comparisons are very difficult due to matrix differences. However, the large increase in strain-to-failure observed in the present study does not appear to take place with carbon black.[38] Cellulose nanofibrils certainly have better reinforcement potential than carbon black due to higher aspect ratio. Previous attempts to use microcrystalline cellulose as reinforcement in polymer composites[39–43] have not produced as strong reinforcement effects as in the present nanocomposite. The scale of the microcrystalline cellulose was typically in the order of tens of micrometers and above, and the shape was in the form of particles. In particular, all the mentioned studies observed decreased strain-to-failure in their composites. It is likely that the less successful reinforcement effects are due to micro- rather than nanoscale dispersion of the microcrystalline cellulose. The more recent study by Cao et al.[7] is based on combination of well-dispersed acid-hydrolyzed nanocellulose with thermoplastic polyurethane particles also dispersed in water. The nanocomposite material of the lowest cellulose content does not show network reinforcement and is comparable with the present material. Interestingly, the reinforcement effect is much lower than in the present case and the strain-to-failure is decreased by nanocellulose addition. The

Table 1. Mechanical Properties of Polyurethane and Polyurethane−Cellulose Composites

	Young's modulus (MPa)			tensile strength (MPa)		strain-to-failure (%)	
sample	experimental	predictions Hui and Shia[a]	predictions Halpin-Tsai[b]	true	engineering	true	engineering
PU	4.9			39	8	159	390
PU/L-C5	6.3			31	9	122	240
PU/C3	7.4	9.8	7.8	83	13	186	540
PU/C5	12.9	12.9	9.8	257	24	237	970
PU/C10	21.1	21.1	15.3	212	24	218	785

[a] Hui and Shia.[44] [b] Halpin-Tsai.[36]

reason may be improved PU−cellulose interaction in the present materials due to reactions between isocyanate and the cellulose hydroxyls.

The increased strain-to-failure in the present nanocomposites and the corresponding high strength is interesting because rubber microcomposites commonly show reduced strain-to-failure with addition of stiff particles or fibers. In addition, at 5 wt % of cellulose, the modulus is twice as high for the nanocomposite as for the microcomposite. These observations are consistent with those for polyurethanes reinforced by layered silicates [11,15–17] The strain-to-failure was substantially increased also in a comparable clay-reinforced thermoplastic polyurethane system.[18] The largest increase (1.3-fold) was recorded for PU containing 1 wt % clay filler. The clays were functionalized with an increasing density of hydroxyl groups. The clays of highest hydroxyl functionality showed the best mechanical properties. The silicate platelets were interpreted to function as chain extenders with positive effects on the physical polyurethane network.

Sternstein and Zhu present interesting data and arguments in a recent paper on the reinforcement mechanism in rubbery matrix thermoplastic nanocomposites.[9] They point out limitations with micromechanics models for prediction of increased modulus with filler content (no size effect). They also emphasize the importance of surface treatment effects on modulus (not expected from micromechanics). Instead, they argue that the reinforcement effects are due to chain bonding to the filler surface. This is the cause of trapped entanglements and enhanced non-Gaussian chain behavior. The argument is based on rubber elasticity theory and stiffness enhancement through entropy effects. Interaction between chain molecules and the filler surface decreases the effective average molar mass between chain entanglements, and therefore modulus increases. In the present case, polyurethane molecule interaction with cellulose nanofibril surfaces may originate from both covalent bonding and secondary interactions such as hydrogen bonding. Stronger interfacial interaction may cause the improved reinforcement effects as compared with water-borne polyurethane nanocomposites.[7]

In Table 1, modulus predictions based on micromechanics models are also included. Predictions based on Hui and Shia[44] and an assumption of random-in-the-plane fiber orientation[36] have been fit to data. Note that Halpin-Tsai[36] predictions are significantly lower. The large modulus difference between matrix and fiber is not properly taken into account in the Halpin-Tsai model, as discussed by Hui and Shia.[44] The cellulose modulus was estimated to 100 GPa along the nanofibril and 4 GPa transverse. A fibril aspect ratio of 22.5 then provides a reasonably good fit. On the basis of the present preparation procedure, a random-in-space fiber architecture seems more likely than the random-in-the-plane assumption on which predictions in Table 1 are based. If the composites indeed have random-in-space fiber architecture, then the rubber elasticity effect is the dominating reinforcement mechanism. The reason is that micromechanics predictions based on random-in-space fiber architecture and reasonable fiber aspect ratio would be much lower than experimental data in Table 1.

Conclusions

High tensile strength and high strain-to-failure nanocomposites with strongly improved modulus were synthesized based on microcrystalline cellulose and polyurethane. A procedure for solvent casting of cellulose nanocomposites based on dry MCC was developed using a thermoplastic polyurethane elastomer. Cellulose dissolution was avoided while still allowing successful dispersion of the cellulose nanofibrils present in dry microscale MCC powder particles. TEM and XRD confirmed the presence of dispersed cellulose nanofibrils. The composition with 5 wt % cellulose was optimal and showed the highest strain-to-failure.

Reinforcement effects are due both to micromechanical effects from stiff nanofibrils in a rubbery matrix and entropic effects from polyurethane molecules interacting physically and chemically with cellulose nanofibril surfaces. The last mechanism is important in cellulose−rubber systems with nanocellulosics as a discrete reinforcement phase rather than as a nanofibrous network.

FT-IR data indicate covalent bonds between cellulose nanofibrils and polyurethane, although hydrogen bonding is also likely to provide strong interaction. With respect to the improvements in ultimate properties (strain-to-failure and strength), cellulose therefore functions like a chain extender and cross-linking agent for polyurethane molecules, analogous to previous observations on silicate platelet nanocomposites, and increase the density of trapped entanglements in the physical network. Because of strong nanofibril−polyurethane interaction at the interface, and corresponding effects on physical network structure, the present nanocomposite has large strain-to-failure. At high strains, cellulose nanofibrils as well as polymer molecules become strongly reoriented in the loading direction, providing additional stiffening.

References and Notes

(1) Okada, A.; Kawasumi, M.; Usuki, A.; Kojima, Y.; Kurauchi, T.; Kamigaito, O. *Mater. Res. Soc. Symp. Proc.* **1990**, *171*, 45.
(2) Sakurada, I.; Nukushina, Y.; Ito, I. *J. Polym. Sci.* **1962**, *57*, 651.
(3) Wainwright, S. A.; Biggs, W. D.; Currey, J. D.; Gosline, J. M. *Mechanical Design in Organisms*, 1st ed.; Princeton University Press: Princeton, 1982; pp 94–95.
(4) Favier, V.; Chanzy, H.; Cavaille, J. Y. *Macromolecules* **1995**, *28*, 6365.
(5) Boldizar, A.; Klason, C.; Kubat, J.; Näslund, P.; Saha, P. *Int. J. Polym. Mater.* **1987**, *11*, 229.
(6) Battista, O. A. *Microcrystal Polymer Science*, 1st ed.; McGraw Hill: New York, 1975; Chapter 2.
(7) Cao, X.; Dong, H.; Li, C. M. *Biomacromolecules* **2007**, *8*, 899.
(8) Wu, Q.; Liu, X.; Berglund, L. A. Polymer nanocomposites based on cellulose. In *23rd Risø International Symposium on Material Science: Sustainable Natural and Polymeric Composites: Science and Technology*; Lilholt, H., Madsen, B., Toftegaard, H. L., Cendre, E., Megnis, M., Mikkelsen, L. P., Sørensen, B. F., Eds.; Risø National Lab: Roskilde, Denmark, 2002; p 107.

(9) Sternstein, S. S.; Zhu, A. J. *Macromolecules* **2002**, *35*, 7262.
(10) Marcovich, N. E.; Auad, M. L.; Bellesi, N. E.; Nutt, S. R.; Aranguren, M. I. *J. Mater. Res.* **2006**, *21*, 870.
(11) Zilg, C.; Thomann, R.; Mülhaupt, R.; Finter, J. *Adv. Mater.* **1999**, *11*, 49.
(12) Demharter, S.; Rösch, J.; Mülhaupt, R. *Polym. Bull.* **1993**, *31*, 421.
(13) Hiljanen-Vainio, M.; Heino, M.; Seppälä, J. V. *Polymer* **1998**, *39*, 865.
(14) Torro-Palau, A.; Fernandez-Garcia, J. C.; Orgiles-Barcelo, A. C.; Pastor-Blas, M. M.; Martin-Martinez, J. M. *J. Adhes. Sci. Technol.* **1997**, *11*, 247.
(15) Chen, T. K.; Tien, Y. I.; Wei, K. H. *Polymer* **2000**, *41*, 1345.
(16) Wang, Z.; Pinnavaia, T. J. *Chem. Mater.* **1998**, *10*, 3769.
(17) Tien, Y. I; Wei, K. H. *Polymer* **2001**, *42*, 3213.
(18) Tien, Y. I.; Wei, K. H. *Macromolecules* **2001**, *34*, 9045.
(19) Gunter, O. *Polyurethane Handbook*, 1st ed.; Macmillan Publishing Co.: New York, 1985; p 453.
(20) Hertzberg, R. W. *Deformation and Fracture Mechanics of Engineering Materials*, 3rd ed.; John Wiley & Sons: New York, 1989.
(21) Rao, C. P.; Balaramm, P.; Rao, C. N. R. *J. Chem. Soc., Faraday Trans. 1* **1980**, *76*, 1008.
(22) El-Kafrawy, A. J. *Appl. Polym. Sci.* **1982**, *27*, 2435.
(23) Dawsey, T. R.; McCormick, C. L. *J. Macromol. Sci., Rev. Macromol. Chem. Phys.* **1990**, *C30*, 405.
(24) Morgenstern, B.; Kammer, H. W. *Trends Polym. Sci.* **1996**, *4*, 87.
(25) Rosenau, T.; Potthast, A.; Hofinger, A.; Sixta, H.; Kosma, P. *Holzforschung* **2001**, *55*, 661.
(26) Potthast, A.; Rosenau, T.; Buchner, R.; Röder, T.; Ebner, G.; Bruglachner, H.; Sixta, H.; Kosma, P. *Cellulose* **2002**, *9*, 41.
(27) Warwicker, J. O.; Wright, A. C. *J. Appl. Polym. Sci.* **1967**, *11*, 659.
(28) Davis, W. E.; Barry, A. J.; Peterson, F. C.; King, A. J. *J. Am. Chem. Soc.* **1943**, *65*, 1294.
(29) Turbak, A. F.; El-Kafrawy, A.; Snyder, F. W.; Auerbach A. B. U.S. Patent 4,302,252, 1981;U.S. Patent 4,352,770, 1982.
(30) Wada, M.; Sugiyama, J.; Okano, T. *J. Appl. Polym. Sci.* **1993**, *49*, 1491.
(31) Tsagaropoulos, G.; Eisenberg, A. *Macromolecules* **1995**, *28*, 6067.
(32) Dufresne, A. *Compos. Interfaces* **2000**, *7*, 53.
(33) Wen, T. C.; Fang, J. C.; Lin, H. J.; Yang, C. H. *J. Appl. Polym. Sci.* **2001**, *82*, 389.
(34) Ferry, A.; Jacobsson, P.; van Heumen, J. D.; Stevens, J. R. *Polymer* **1996**, *37*, 737.
(35) Woods, G. *The ICI Polyurethanes Book*, 2nd ed.; John Wiley & Sons: New York, 1990.
(36) Hull, D. *An Introduction to Composite Materials*, 1st ed.; Cambridge Solid State Science Series; Cambridge University Press: Cambridge, U.K., 1993; pp 87−91, 150.
(37) Sjögren, B. A.; Berglund, L. A. *Polym. Compos.* **1999**, *20*, 705.
(38) Kraus, G. *Rubber Chem. Technol.* **1965**, *38*, 1070.
(39) Maskavs, M.; Kalnins, M.; Laka, M.; Chernyavskaya, S. *Mech. Compos. Mater.* **2001**, *37*, 159.
(40) Laka, M. S.; Chernyavskaya, L.; Faitelson, A. *Cellul. Chem. Technol.* **2003**, *37*, 69.
(41) Laka, M.; Chernyavskaya, S.; Maskavs, M. *Mech. Compos. Mater.* **2003**, *39*, 183.
(42) Borges, J. P.; Godinho, M. H.; Martins, A. F.; Stamatialis, D. F.; De Pinho, M. N.; Belgacem, M. N. *Polym. Compos.* **2004**, *25*, 102.
(43) Mathew, A. P.; Oksman, K.; Sain, M. *J. Appl. Polym. Sci.* **2005**, *97*, 2014.
(44) Hui, C. Y.; Shia, D. *Polym. Eng. Sci.* **1998**, *38*, 774.

BM701061T